

# Molecular dynamics studies of $\alpha$ -helix stability in fibril-forming peptides

Erik Nordling · Yvonne Kallberg · Jan Johansson ·  
Bengt Persson

Received: 21 January 2007 / Accepted: 17 November 2007 / Published online: 6 December 2007  
© Springer Science+Business Media B.V. 2007

**Abstract** Diseases associated with protein fibril-formation, such as the prion diseases and Alzheimer's disease, are gaining increased attention due to their medical importance and complex origins. Using molecular dynamics (MD) simulations in an aqueous environment, we have studied the stability of the  $\alpha$ -helix covering positions 15–25 of the amyloid  $\beta$ -peptide (A $\beta$ ) involved in Alzheimer's disease. The effects of residue replacements, including the effects of A $\beta$  disease related mutations, were also investigated. The MD simulations show a very early (2 ns) loss of  $\alpha$ -helical structure for the Flemish (A $\beta$ (A21G)), Italian (A $\beta$ (E22K)), and Iowa (A $\beta$ (D23N)) forms associated with hereditary Alzheimer's disease. Similarly, an early (5 ns) loss of  $\alpha$ -helical structure was observed for the Dutch (A $\beta$ (E22Q)) variant. MD here provides a possible explanation for the structural changes. Two variants of A $\beta$ , A $\beta$ (K16A,L17A,F20A) and A $\beta$ (V18A,F19A,F20A), that

do not produce fibrils in vitro were also investigated. The A $\beta$ (V18A,F19A,F20A) initially loses its helical conformation but refolds into helix several times and spends most of the simulation time in helical conformation. However, the A $\beta$ (K16A,L17A,F20A) loses the  $\alpha$ -helical structure after 5 ns and does not refold. For the wildtype A $\beta$ (1–40) and A $\beta$ (1–42), the helical conformation is lost after 5 ns or after 40 ns, respectively, while for the “familial” (A $\beta$ (A42T)) variant, the MD simulations suggest that a C-terminal  $\beta$ -strand is stabilised, which could explain the fibrillation. The simulations for the Arctic (A $\beta$ (E22G)) variant indicate that the  $\alpha$ -helix is kept for 2 ns, but reappears 2 ns later, whereafter it disappears after 10 ns. The MD results are in several cases compatible with known experimental data, but the correlation is not perfect, indicating that multimerisation tendency and other factors might also be important for fibril formation.

E. Nordling  
Department of Medical Biochemistry and Biophysics,  
Karolinska Institutet, Stockholm 171 77, Sweden

E. Nordling (✉)  
Biovitrum AB, Stockholm 117 62, Sweden  
e-mail: erik.nordling@biovitrum.com

Y. Kallberg · B. Persson  
IFM Bioinformatics, Linköping University, Linköping 581 83,  
Sweden

Y. Kallberg · B. Persson  
Department of Cell and Molecular Biology, Karolinska  
Institutet, Stockholm 171 77, Sweden

J. Johansson  
Department of Anatomy, Physiology and Biochemistry, Swedish  
University of Agricultural Sciences, The Biomedical Centre,  
Uppsala 751 23, Sweden

**Keywords** Amyloid  $\beta$ -peptide · Amyloid fibril ·  
Molecular dynamics · Secondary structure

## Abbreviations

A $\beta$  Amyloid  $\beta$ -peptide  
MD Molecular dynamics

## Introduction

Amyloid fibril-formation as a cause of disease has gained increased attention due to the prion diseases, bovine spongiform encephalopathy and the human counterpart Creutzfeldt-Jakob's disease [1]. Another amyloid disease is Alzheimer's disease, of importance in dementia among

an aging population. Presently, over 20 diseases, systemic or localised to various organs are associated with fibril formation [2]. These diseases have in common that endogenous proteins act as potential pathogenic agents. The fibril-forming proteins share no known patterns in sequence or structure, e.g. they range from all-helical to all-sheet proteins. However, they appear to have a common tendency to unfold and assume a conformation that can multimerise and form inter-molecular  $\beta$ -sheets that can grow into insoluble fibrils [3]. The neuronal toxicity in Alzheimer's disease is thought to originate from the extracellular neuronal plaques that are created by the fibril-forming amyloid  $\beta$ -peptide ( $A\beta$ ) [4], but recent studies indicate that soluble  $A\beta$  oligomers, also known as ADDLs ( $A\beta$ -derived diffusible ligands) may also be toxic [5]. ADDLs appear spontaneously in human brain cells [6], and in transgenic mice  $A\beta$  accumulates intracellularly and cause neurodegeneration prior to amyloid plaque formation [7]. Recently, a 56 kDa oligomer of  $A\beta$ , dubbed  $A\beta^*$  56, was shown to associate with memory loss in transgenic mice [8]. Also oligomeric fibrillar structures, but not mature fibrils, formed from proteins that are not associated with disease are cytotoxic, suggesting that the toxicity is not protein-specific but mediated by the oligomeric fibrillar structure as such [9]. The toxicity of  $A\beta$  is coupled to the loss of the native structure [10]. Irrespective of the exact nature of the toxic form(s) of  $A\beta$ , they most likely require loss of the helical structure and formation of  $\beta$ -sheet structure.

Some fibril-forming proteins contain discordant  $\alpha$ -helices, which are composed of a stretch of amino acid residues that statistically are predicted to be found in an extended conformation [11]. These proteins include the prion protein and  $A\beta$ . The occurrence of discordant helices in fibril-forming proteins indicates that destabilising factors are present in their amino acid sequences. Replacement of the  $\beta$ -preferring amino acid residues in some of the discordant helices has been shown to change the potential to form fibrils. In  $A\beta$ , replacing Val18 with Ala, or Lys16, Leu17 and Phe20 with Ala, or replacing Val18, Phe19 and Phe20 with Ala prevents fibril formation [12–14]. In this study, molecular dynamics (MD) simulations were used to study the influence of the amino acid sequences of the  $A\beta$  variants on the stabilities of their respective helices.

The  $A\beta$  mutations that are associated with hereditary cerebral haemorrhage with amyloidosis of the Dutch type ( $A\beta$ (E22Q); [15]) and the Italian type ( $A\beta$ (E22K); [16]), like  $A\beta$ (E22Q) have been shown to fibrillate fast in vitro while  $A\beta$ (E22K) is similar to wild-type  $A\beta$  in fibrillation velocity [16]. Hereditary cerebroarterial amyloidosis of the Iowa type ( $A\beta$ (D23N)) has an onset in the 6th or 7th decade of life [17] and the peptide displays fast fibrillation

in vitro [18]. Hereditary cerebral amyloidosis of the Flemish ( $A\beta$ (A21G); [19]) and the Arctic ( $A\beta$ (E22G); [20]) types both have an onset in the 5th decade of life [19, 20].  $A\beta$ (E22G) shows fast fibril formation in model systems [21], while  $A\beta$ (A21G) mainly increases the rate of secretion of  $A\beta$ -peptide [18]. Finally a mutation adjacent to the  $\gamma$ -secretase cleavage site associated with familial Alzheimer disease ( $A\beta$ (A42T); [22]) was included in the study. This mutation has not been reported to increase the fibrillation velocity but rather to alter the cleavage of the  $A\beta$  precursor and influence the ratio of  $A\beta$ 1–40 to  $A\beta$ 1–42 [23].

Two  $A\beta$  variants that do not fibrillate under the same conditions as wild-type  $A\beta$ ,  $A\beta$ (K16A,L17A,F20A) [13] and  $A\beta$ (V18A,F19A,F20A) [14] were also included in the simulations.

## Materials and methods

The conformation of  $A\beta$  was taken from the NMR structure (PDB-code 1ba6, [24]). The mutated forms were constructed from the  $A\beta$ (1–42) peptide by initially giving the replaced residues the same rotamer as the original counterpart. Unfavourable contacts introduced by the substitution were relieved by a 1,000 steps conjugate gradient minimisation of the side-chains. The replacement and the following minimisations were carried out using ICM (Molsoft LLC, San Diego, Calif.).

MD simulations were performed using the GROMACS molecular dynamics program, version 3.31 [25] with the OPLS-AA force field [26]. The simulations were executed with explicit water molecules, using the simple point charge model for the water molecules [27]. The temperature was kept constant during the simulations using a Berendsen thermostat [28] with a coupling time of 0.1 ps. The pressure was maintained by coupling to a reference pressure of 1 bar with a coupling time of 1 ps and an isothermal compressibility of  $4.5 \times 10^{-5} \text{ bar}^{-1}$ . A twin range cut-off of 0.8 and 1.4 nm was used for the evaluation of the non-bonded interactions. Interactions within the larger cut-off were updated every 10 steps. The time step used was 2 fs. The simulations lasted for 100 ns and were carried out at 310 K.

To judge whether the simulations had reached a level of equilibrium, the potential energy and the root mean squared distance (RMSD) were plotted versus the simulation time. The RMSD is calculated based on all atoms in the peptide after it has been superimposed upon the original structure as implemented in the GROMACS package [25]. The individual simulations were then evaluated by calculating secondary structure content for the peptides for each 500:th ps of the entire simulation with the DSSP algorithm [29].

The statistical preference for each peptide to form  $\alpha$ -helix or  $\beta$ -strand was calculated based upon the propensity values calculated from the fractional occurrences of residues in different secondary structures in 1,091 proteins [11]. For each residue, the value was calculated by averaging the propensities for all residues within a five-residue window centred on the residue in question.

## Results

### MD simulations of A $\beta$ and analogues

The potential energy for the system is plotted for the entire calculation in Fig. 1a, worth noting is that A $\beta$ (1–40) has a higher energy even though the total size of that system is smaller. The potential energy of all simulations is stable during the entire calculation. In Fig. 1b the RMSD versus the starting conformation is plotted against the simulation time. After 20 ns all simulations are within a span of 0.9–1.4 nm in RMSD from the original structure. The variant that diverts fastest from the original structure is A $\beta$ (D23N) which has diverted to its maximum RMSD compared to the native structure during the initial 5–10 ns of the simulation.

In Fig. 2, the secondary structure states every 500:th ps for all peptides are plotted against the simulation time. The wild-type A $\beta$ (1–40) (Fig. 2a) and A $\beta$ (1–42) (Fig. 2b) differ by that the longer form maintains a helical region for about 40 ns of the simulation, while the shorter form loses the central helical region after approximately 5 ns. A $\beta$ (1–40) also displays more  $\beta$ -sheet regions than A $\beta$ (1–42).

For A $\beta$ (A21G) (Fig. 2c) a disruption of the helical region is observed already during the first 5 ns. An unordered region is also clearly centered upon the mutation-site for most of the simulation. The initially  $\alpha$ -helical region refolds into a  $3_{10}$  helix, disrupted by the mutant glycine residue. A few ns long  $\beta$ -sheets are also visible.

A $\beta$ (E22G) (Fig. 2d) shows an unordered region originating around the mutation-site. The first part of the helix is kept intact for the first 2 ns of the simulation, but reappears 2 ns later. However, after 10 ns there is no helical content. A $\beta$ (E22Q) (Fig. 2e) maintains the original extent of the helical central region for approximately 5 ns. For A $\beta$ (E22K) (Fig. 2f) the substitution seems to affect the local helical content rapidly, as the C-terminal part of the helix unwinds after 2 ns, but the N-terminal part of the helix is conserved and extended somewhat over time.

The A $\beta$ (D23N) (Fig. 2g) assumes a more or less random conformation after 1 ns of the simulation.

For A $\beta$ (A42T) (Fig. 2h) the central helical region is maintained for 11 ns and parts of it are restored during the simulation, but the substitution of the last amino acid

residue appears to stabilise an intra-molecular  $\beta$ -sheet in the C-terminal part, which appears after 40 ns of the simulation and reoccurs multiple times during the simulation, lasting for periods of up to 7 ns.

The two designed non fibril forming variants, A $\beta$ (K16A, L17A, F20A) (Fig. 2i) and A $\beta$ (V18A, F19A, F20A) (Fig. 2j) behave in different manners. The first one loses its helical region after 5 ns and does not refold, while the latter fast loses its helical conformation but refolds into a helix several times and spends most of the simulation time including the last 30 ns in a helical conformation.

### Secondary structure propensities

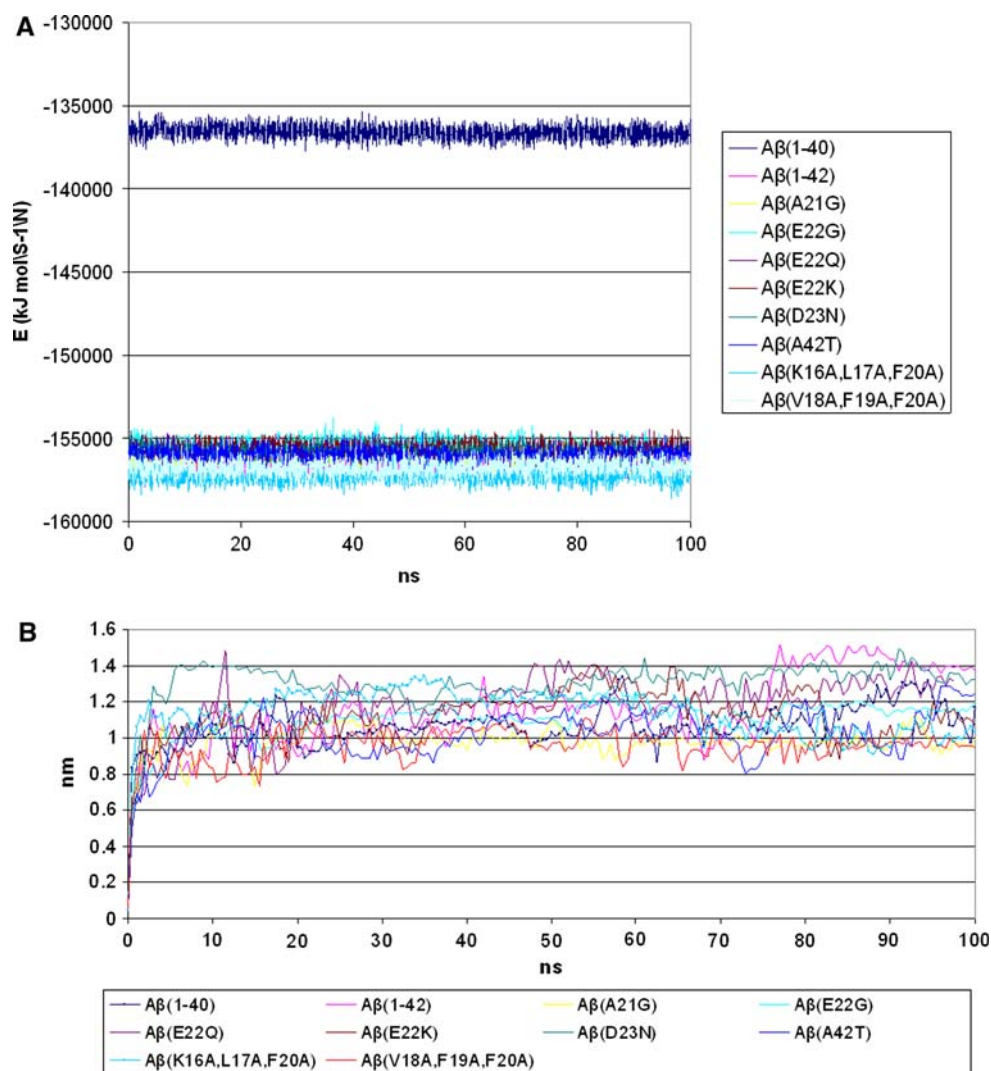
Secondary structure preferences, expressed as the quotient of  $\alpha$ -helix propensity over  $\beta$ -strand propensity, for the A $\beta$  variants studied herein are shown in Fig. 3. As expected, the analogues A $\beta$ (K16A, L17A, F20A) and A $\beta$ (V18A, F19A, F20A) both show substantially increased preferences for helical structure compared to wild-type A $\beta$ . The disease related mutant forms of A $\beta$  show a decreased helix/strand quotient compared to A $\beta$ (1–42), in particular A $\beta$ (A21G) and A $\beta$ (E22G).

## Discussion

In this study MD simulations were used to investigate the stability of the helical form of A $\beta$  and analogues of it with altered potential to form fibrils. A $\beta$  is a cleavage product of the transmembrane amyloid precursor protein (APP), and the region containing the helix now investigated (residues 15–25) is located just N-terminally to the predicted membrane-spanning region starting at residue 29 [30]. A $\beta$  is structurally flexible in aqueous solution [31] but the central helix is stabilised in the presence of trifluoroethanol and detergent micelles [32]. The simulations of A $\beta$ (1–40) and A $\beta$ (1–42) hint that A $\beta$ (1–42) has a more stable central helical region during the time of the simulation. This is surprising as A $\beta$ (1–42) is more prone to form fibrils compared to A $\beta$ (1–40). NMR experiments have previously reported that A $\beta$ (1–40) and A $\beta$ (1–42) have similar helical stability [31], which could indicate that the results from the MD simulations reflect that neither of the peptides is particularly stable. It was recently proposed that a major difference between A $\beta$ (1–40) and A $\beta$ (1–42) is that A $\beta$ (1–42) forms trimers and tetramers more favourably than A $\beta$ (1–40) [33]. A more favourable oligomerisation of A $\beta$ 1–42 may drive fibril formation.

The non-fibrillating variants A $\beta$ (K16A, L17A, F20A) and A $\beta$ (V18A, F19A, F20A) appear to resist fibrillation via different mechanisms. A $\beta$ (K16A, L17A, F20A)

**Fig. 1** (a) Potential energy of the system during the 100 ns simulation. (b) RMSD in nm of all atoms during the 100 ns simulation compared to the original conformation



remains in a helical conformation for 5 ns after which it adopts a more random conformation centrally. Its resistance to fibril formation can be linked to a reduced ability to form intermolecular hydrogen bonds, as was the rationale behind its design [13]. Replacing large amino acid residues like Lys, Leu and Phe with the conformationally less strained Ala could add flexibility to the helix, which may result in a less stable helix in the simulations. This could also make the coil to  $\beta$ -sheet transformation in the fibrillation process more unfavourable, as more entropy is lost. In A $\beta$ (V18A,F19A,F20A), the replacement of the  $\beta$ -sheet preferring residues with the  $\alpha$ -helical preferring alanine appears to allow the peptide to re-enter an  $\alpha$ -helical conformation during the simulation.

The apparent stability of A $\beta$ (E22Q) in the simulations is unexpected since it has been reported to fibrillate fast in vitro [16]. One possibility is that removal of a negative charge close to Asp23, which has been shown to form a

salt-bridge in A $\beta$  fibrils, may ease the correct matching of the salt-bridge that stabilises the bend in the fibrils [34], which in turn could speed up the fibrillation process. Another possibility is that the mutation leads to a lower solubility of the peptide compared to wild-type A $\beta$ , which also should increase the velocity of the fibrillation process [35]. A $\beta$ (E22G) (Fig. 2d) and A $\beta$ (D23N) (Fig. 2g) both show high fibrillation rates and aggressive fibrillation [18, 20, 21], which seems to match their low helical stability in the simulations.

A $\beta$ (E22K) forms fibrils with similar kinetics as wild-type A $\beta$  [16] and the simulation show a more stable helical region compared to the wild-type (Fig. 2f). The simulation of A $\beta$ (A42T) shows that the mutation appears to stabilise the formation of a  $\beta$ -sheet in the C-terminal region, but it also shows a recurring helical segment in the central region (Fig. 2h), which may act as a counterweight to fibrillation for this peptide. Previously it has been suggested that A $\beta$ (A42T) primarily induce amyloidosis by influencing the



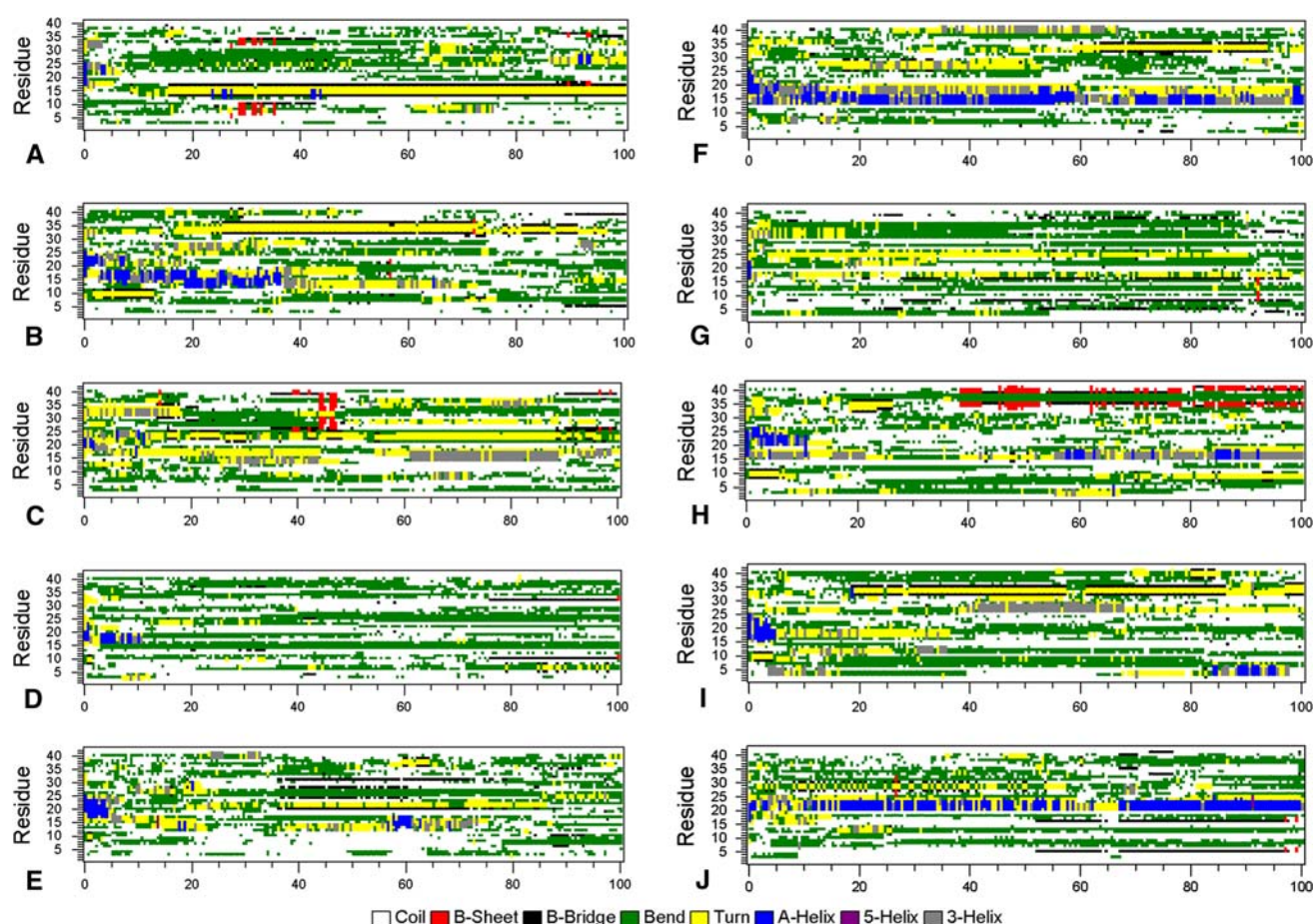
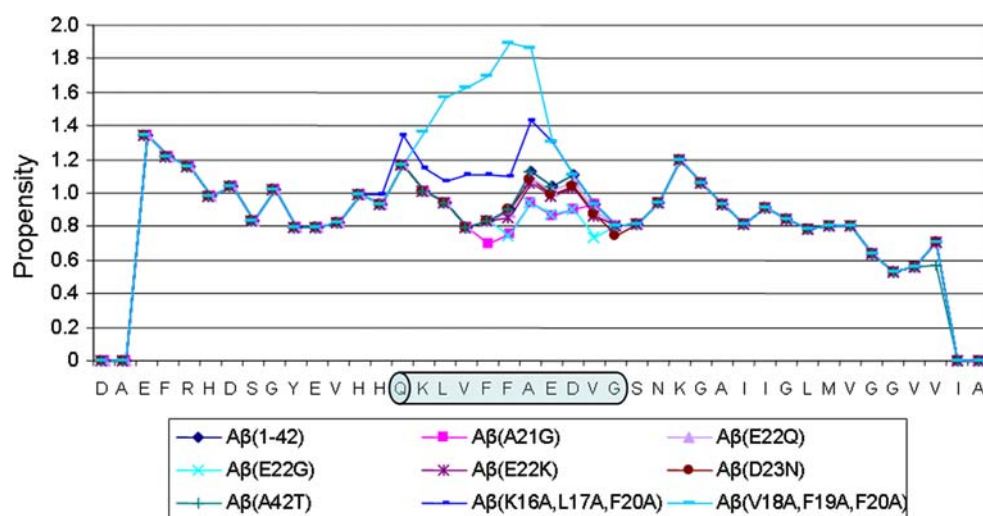


**Fig. 2** A visualisation of the secondary structure of the simulations during the 100 ns simulations for (a) A $\beta$ (1–40), (b) A $\beta$ (1–42), (c) A $\beta$ (A21G), (d) A $\beta$ (E22G), (e) A $\beta$ (E22Q), (f) A $\beta$ (E22K), (g) A $\beta$ (D23N),

(h) A $\beta$ (A42T), (i) A $\beta$ (K16A,L17A,F20A) and (j) A $\beta$ (V18A,F19A,F20A)

**Fig. 3** Quotient of  $\alpha$ -helix propensity and  $\beta$ -strand propensity for A $\beta$  and analogues thereof. The helix in the PDB-structure of A $\beta$  is marked with a cylinder. A $\beta$ 1–40 is not shown as the propensity is equal to A $\beta$ 1–42 for the entire length of the sequence



cleavage of APP and the ratio between A $\beta$ (1–40) and A $\beta$ (1–42) [23]. The A $\beta$ (A21G) mutant is one of the most unstable peptides during the simulations, with a break-up of the central helical region after just 1 ns and the

appearance of a C-terminal  $\beta$ -sheet that lasts 2 ns at a time. However, the A $\beta$ (A21G) mutation has been reported not to increase the fibrillation rate [18, 36] but instead increase the rate of release of A $\beta$  [18]. Van Nostrand et al. [18] did

note a pronounced neurotoxicity of A $\beta$ (A21G), which suggests that the observed low helical stability of A $\beta$ (A21G) could promote formation of toxic oligomers.

Whether helical instability is important for A $\beta$  fibril formation in vivo needs to be investigated further. Additional effects of the mutations, like increased potential to form  $\beta$ -sheets and reduced solubility, are not addressed by the current simulations. Also, possible interactions between multiple A $\beta$  molecules have not been considered in this study, due to computational time restraints. In spite of these caveats, the MD results suggest that helix destabilisation should be considered as one potential mechanism associated with mutations in the central part of A $\beta$ .

Overall, the MD simulations are compatible with the idea that stabilisation of helices in peptides/proteins involved in amyloid diseases affect the potential to form fibrils. Stabilising a helical monomeric conformation may be more attractive than to inhibit fibril growth by preventing  $\beta$ -sheet formation [37, 38], since the latter may result in an increased amount of potentially toxic A $\beta$  oligomers.

**Acknowledgements** Financial support from the Swedish Research Council, the Swedish Foundation for Strategic Research, Linköping University and Karolinska Institutet Funds is gratefully acknowledged.

## References

- Jackson GS, Collinge J (2001) *Mol Pathol* 54:393
- Westermarck P (2005) *FEBS J* 272:5942
- Nelson R, Eisenberg D (2006) *Curr Opin Struct Biol* 16:260
- Lorenzo A, Yankner BA (1996) *Ann NY Acad Sci* 777:89
- Lambert MP, Barlow AK, Chromy BA, Edwards C, Freed R, Liosatos M, Morgan TE, Rozovsky I, Trommer B, Viola KL, Wals P, Zhang C, Finch CE, Krafft GA, Klein WL (1998) *Proc Natl Acad Sci USA* 95:6448
- Walsh DM, Tseng BP, Rydel RE, Podlisny MB, Selkoe DJ (2000) *Biochemistry* 39:10831
- Chui DH, Tanahashi H, Ozawa K, Ikeda S, Checler F, Ueda O, Suzuki H, Araki W, Inoue H, Shirotani K, Takahashi K, Gallyas F, Tabira T (1999) *Nat Med* 5:560
- Lesne S, Koh MT, Kotilinek L, Kaye R, Glabe CG, Yang A, Gallagher M, Ashe KH (2006) *Nature* 440:352
- Bucciantini M, Giannoni E, Chiti F, Baroni F, Formigli L, Zurdo J, Taddei N, Ramponi G, Dobson CM, Stefani M (2002) *Nature* 416:507
- Monji A, Utsumi H, Ueda T, Imoto T, Yoshida I, Hashioka S, Tashiro K, Tashiro N (2001) *J Neurochem* 77:1425
- Kallberg Y, Gustafsson M, Persson B, Thyberg J, Johansson J (2001) *J Biol Chem* 276:12945
- Soto C, Castano EM, Frangione B, Inestrosa NC (1995) *J Biol Chem* 270:3063
- Tjernberg LO, Naslund J, Lindqvist F, Johansson J, Karlstrom AR, Thyberg J, Terenius L, Nordstedt C (1996) *J Biol Chem* 271:8545
- Paivio A, Nordling E, Kallberg Y, Thyberg J, Johansson J (2004) *Protein Sci* 13:1251
- Levy E, Carman MD, Fernandez-Madrid JJ, Power MD, Lieberburg I, van Duinen SG, Bots GTAM, Luyendijk W, Frangione B (1990) *Science* 248:1124
- Miravalle L, Tokuda T, Chiarle R, Giaccone G, Bugiani O, Tagliavini F, Frangione B, Ghiso J (2000) *J Biol Chem* 275:27110
- Grabowski TJ, Cho HS, Vonsattel JPG, Rebeck GW, Greenberg SM (2001) *Ann Neurol* 49:697
- van Nostrand WE, Melchor JP, Cho HS, Greenberg SM, Rebeck GW (2001) *J Biol Chem* 276:32860
- Hendriks L, van Duijn CM, Cras P, Cruts M, Van Hul W, van Harskamp F, Warren A, McInnis MG, Antonarakis SE, Martin J-J, Hofman A, Van Broeckhoven C (1992) *Nat Genet* 1:218
- Kamino K, Orr HT, Payami H, Wijsman EM, Alonso ME, Pulst SM, Anderson L, O'dahl S, Nemens E, White JA, Sadovnick AD, Ball MJ, Kaye J, Warren A, McInnis M, Antonarakis SE, Korenberg JR, Sharma V, Kukull W, Larson E, Heston LL, Martin GM, Bird TD, Schellenberg GD (1992) *Am J Hum Genet* 51:998
- Cheng IH, Palop JJ, Esposito LA, Bien-Ly N, Yan F, Mucke L (2004) *Nat Med* 10:1190
- Carter DA, Desmarais E, Bellis M, Champion D, Clerget-Darpoux F, Brice A, Agid Y, Jaillard-Serradt A, Mallet J (1992) *Nat Genet* 2:255
- Rossi G, Giaccone G, Maletta R, Morbin M, Capobianco R, Mangieri M, Giovagnoli AR, Bizzi A, Tomaino C, Perri M, Di Natale M, Tagliavini F, Bugiani O, Bruni AC (2004) *Neurology* 63:910
- Watson AA, Fairlie DP, Craik DJ (1998) *Biochemistry* 37:12700
- Lindahl E, Hess B, van der Spoel D (2001) *J Mol Model* 7:306
- Kaminski GA, Friesner RA, Tirado-Rives J, Jorgensen WL (2001) *J Chem Phys B* 105:6474
- Berendsen HJC, Postma JPM, van Gunsteren WF, Hermans J (1981) In: Pullman B (ed) *Intermolecular forces*. Reidel, Dordrecht, pp 331–342
- Berendsen HJC, Postma JPM, van Gunsteren WF, DiNola A, Haak JR (1984) *J Chem Phys* 81:3684
- Kabsch W, Sander C (1983) *Biopolymers* 22:2577
- Gasteiger E, Gattiker A, Hoogland C, Ivanyi I, Appel RD, Bairoch A (2003) *Nucleic Acids Res* 31:3784
- Riek R, Guntert P, Dobeli H, Wipf B, Wuthrich K (2001) *Eur J Biochem* 268:5930
- Serpell LC (2000) *Biochim Biophys Acta* 1502:16
- Chen YR, Glabe CG (2006) *J Biol Chem* 281:24414
- Lührs T, Ritter C, Adrian M, Riek-Loher D, Bohrmann B, Dobeli H, Schubert D, Riek R (2005) *Proc Natl Acad Sci USA* 102:17342
- Chiti F, Stefani M, Taddei N, Ramponi G, Dobson CM (2003) *Nature* 424:805
- Murakami K, Irie K, Morimoto A, Ohigashi H, Shindo M, Nagao M, Shimizu T, Shirasawa T (2003) *J Biol Chem* 278:46179
- Gordon DJ, Sciarretta KL, Meredith SC (2001) *Biochemistry* 40:8237
- Watanabe K, Nakamura K, Akikusa S, Okada T, Kodaka M, Konakahara T, Okuno H (2002) *Biochem Biophys Res Commun* 290:121